Kovove Mater. 48 2010 179–184
DOI: 10.4149/km_2010_3_179

An investigation into the effect of welding current on the plasma arc welding of pure titanium

N. Kahraman[1]*, M. Taşkın[2], B. Gülenç[2], A. Durgutlu[3]

[1] *Karabuk University, Technical Education Faculty, 78050 Karabuk, Turkey*
[2] *Fırat University, Technical Education Faculty, 23119 Elazig, Turkey*
[3] *Gazi University, Technical Education Faculty, 06500 Ankara, Turkey*

Received 16 April 2009, received in revised form 17 December 2009, accepted 9 February 2010

Abstract

In the present study, plasma arc welding method was applied to commercial purity titanium using various welding current values. In order to determine the strength of the resulting joints, tensile tests, impact tests and hardness tests were applied. Additionally, optical microscopy examinations were carried out to determine the interface properties of the joints. The work showed that the highest interface strength was obtained for the specimens joined at 65 A. For all the welding parameters, the hardness test results showed that weld metal gave a higher hardness value than heat affected zone and base metal. The microstructure in welded joint consisted of acicular alpha and twins.

K e y w o r d s: plasma arc welding, titanium, welding current

1. Introduction

Titanium and its alloys have been considered as one of the best engineering metals for industrial applications [1–3]. They have been used in a number of applications in industry due to their excellent combination of properties such as elevated strength-to-weight ratio, high fatigue life, toughness, excellent resistance to corrosion, good fatigue strength [4–8], high melting point [9, 10], good high-temperature properties [11, 12]. In addition, some grades of them exhibit good weldability [13]. Commercially pure titanium (CP--Ti) is widely used as dental implant and restorations because of its suitable mechanical properties, excellent corrosion resistance and biocompatibility [14–17]. With the increased use of CP-Ti, the joining of titanium has become more and more important [18, 19].

Although some grades of Ti and its alloys exhibit good weldability, problems are encountered when welding some other grades of Ti and its alloys, as they are extremely chemically reactive at high temperatures [20]. In addition, welding leads to grain coarsening at the fusion zone and heat affected zone (HAZ) [1, 21]. TIG is a usual welding method for joining Ti and its alloys [5, 22, 23]. Another method for joining Ti and its alloys is plasma arc welding. The plasma arc welding (PAW) with high energy density and high welding speed is a new welding method [24].

For the PAW technology, understanding about the characters of the constricted plasma arc is helpful to utilize this kind of processing technology well [25]. The welds are small and more like those found in conventional arc welding [26]. In plasma arc welding, an electric arc is generated between a non--consumable tungsten electrode and the working piece, which is constrained using a copper nozzle with a small opening at the tip. By forcing the plasma gas and arc through a constricted orifice, the torch delivers a high concentration of energy to a small area, giving higher welding speeds and producing welds with high penetration/width ratios, thus limiting the HAZ dimensions [27]. The two outstanding advantages of plasmas are higher temperature and better heat transfer to other objects [28]. The process can be operated with or without a filler wire addition [29, 30]. PAW uses the keyhole method to obtain a full penetration weld [30, 31], narrower weld beads and minimal distortion [32]. PAW is used extensively to weld carbon steel, stainless

*Corresponding author: tel.: +90 370 433 82 00; fax: +90 370 433 82 04; e-mail address: nkahraman@karabuk.edu.tr

Table 1. Chemical composition of the pure Ti sheet (wt.%)

ASTM Standard	Transformation temperatures (°C)		Alloying elements (wt.%)				
	Alpha, α	Beta, β	N	C	H	Fe	O
Grade 2	913	890	0.03	0.10	0.015	0.30	0.25

Table 2. Welding conditions applied for PAW

Welding current (A)	50, 55, 60, 65
Welding speed (cm min^{-1})	15
Orifice gas flow (L min^{-1})	0.5
Shielding gas flow (L min^{-1})	30
Shielding gas nozzle/workpiece distance (mm)	3
Tungsten electrode diameter (mm)	4.7

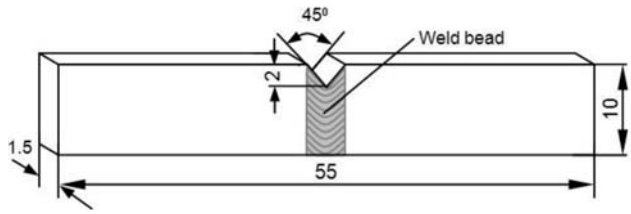

Fig. 1. Impact test specimen.

steel, nickel-based alloys, titanium alloys, aluminium and magnesium alloys [27, 33, 34].

Though there are many reports published on the joining magnesium alloys [35], aluminium alloys [36], iron-based powder metal [32], SiC/Al metal matrix composites [37], and duplex stainless steels [27] by PAW method, there are few studies dealing with welding of Ti and their alloy by PAW process [38–40]. In addition, these studies are quite old. The objective of the present work is to study the effect of the welding current on plasma arc welding of pure titanium. Weld quality of the plasma arc welded specimens were examined by tensile test, impact test, hardness test and microstructural characterization of the joined metals.

2. Materials and experimental procedure

In this study, commercially pure titanium (ASTM Grade 2) sheets were used. The chemical composition of Ti in weight percentages is given in Table 1. The titanium sheets in the dimensions of 100 × 80 × 1.5 mm^3 were welded by PAW method. During welding process, the sheets were butt joint when they were in flat position without filler metal using a single pass metal. The specimen surfaces were chemically cleaned by acetone before the welding in order to eliminate surface contaminations. Pure argon was used as both the shielding gas and plasma gas. Table 2 shows the welding process parameters.

Rectangular tensile test specimens were prepared from the welded joints with the dimensions of 12 × 80 mm^2 as the thickness of the plates was less than 2 mm in order to determine the mechanical properties of the joints, the tensile test (according to standards EN 895) was carried out on the welded specimens with the strain rate of 1.4×10^{-2} s^{-1} using an Autograph-Shimadzu tensile testing machine. The impact samples were prepared as shown in Fig. 1 and were subjected to Standard V notch Charpy test in room temperature using a Devotrans Devo (CDC 0700014) type impact machine. The hardness specimens were mounted in bakelite and then microhardness measurements were performed using a Shimadzu HMV unit under 200 g load.

After the welding process, the welded specimens were cut transversely of the welds and prepared for metallographic inspection by mounting, mechanical polishing and etching in a Kroll reagent to reveal microstructure. A Nikon Epiphot 200 optical microscope was used for the microscopic examination.

3. Results and discussions

3.1. Weld bead

Photos of the welded specimens obtained at four different welding currents (50, 55, 60 and 65 A) by PAW method are given in Fig. 2. Visual examinations of the welded specimens showed that the weld beads were quite smooth. In addition, it is seen from Fig. 2 that increasing welding current increases the weld bead and HAZ. Li et al. [19] stated that bright silver colour of the weld zone and little deformation of the joined parts are the indications of effective shielding of the molten pool in welding Ti.

3.2. Microhardness of the welds

Figure 3 shows Vickers hardness indentations placed across the four welds (from the weld centreline on both sides through the HAZ and into the base metal). The hardness is marginally higher in the weld

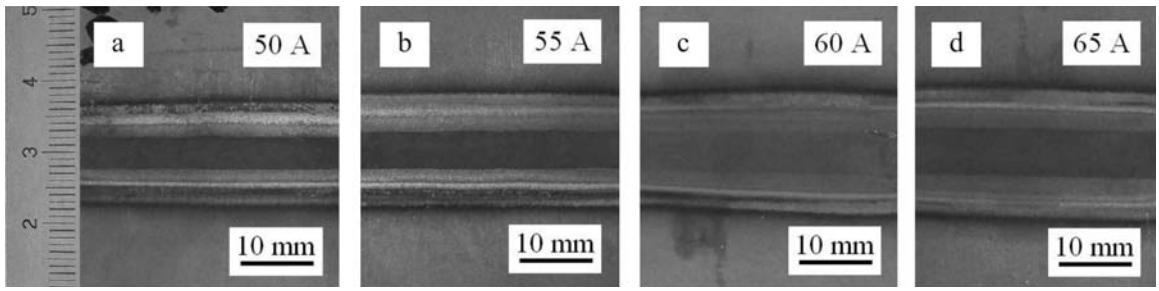

Fig. 2a–d. Top view of the weld beads obtained at different welding currents in PAW.

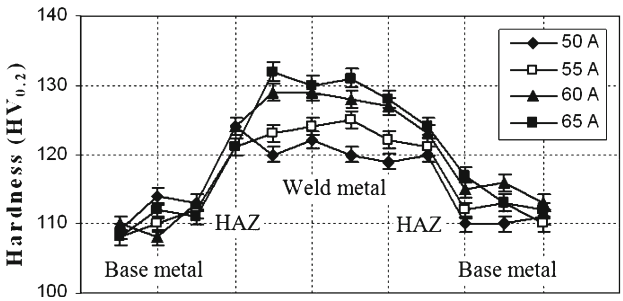

Fig. 3. Microhardness across base metal, HAZ and weld metal (centreline).

metal and HAZ when compared to the base metal. Saresh et al. [8], Li et al. [19] and Yunlian et al. [22] have joined titanium materials by different welding method, and they reported that the highest levels of hardness were obtained for the weld metal, and the hardness decreased as the distance from the weld centre increased on both sides. The average increase of hardness in weld metal is 119–133 HV and in HAZ is 120–126 HV as against the base metal hardness of 108–112 HV.

From Fig. 3 it is clearly seen that welding current affected the hardness of weld zone. It was observed that increasing welding current increased the hardness of weld metal and HAZ. This increase was attributed to oxygen concentration in the weld [19].

3.3. Tensile properties

Figure 4 shows the tensile strength and elongation values of base metal and four welded joints. For the specimens welded at welding currents of 55, 60 and 65 A, fracture took place at the base metal. However, in the case of the specimen welded at 50 A welding current, fracture took place at the weld metal. Figure 5 shows the fracture photos of the specimens after tensile testing.

When Fig. 4 is examined, it is seen that the ultimate tensile strength values of welded specimens are as much as that of the base metal except for the specimen welded at welding current of 50 A. These results can be recognised as acceptable industrially as the strength calculations made in the design of a fabricated structure are based on the properties of the metal being used. Ideally the weld should have properties at least equal to those of the parent metal [26].

It was seen that the specimen welded at 50 A welding current was fractured in the weld bead at a stress value lower than that required to break the base metal. This was attributed to a poor weld penetration due to low heat input at welding current of 50 A. Adequate

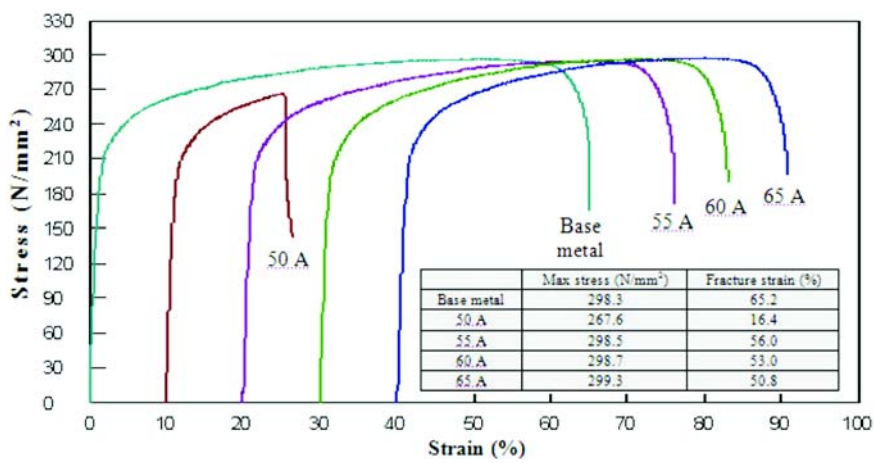

Fig. 4. Tensile strength and elongation values of the base metal and weld joints.

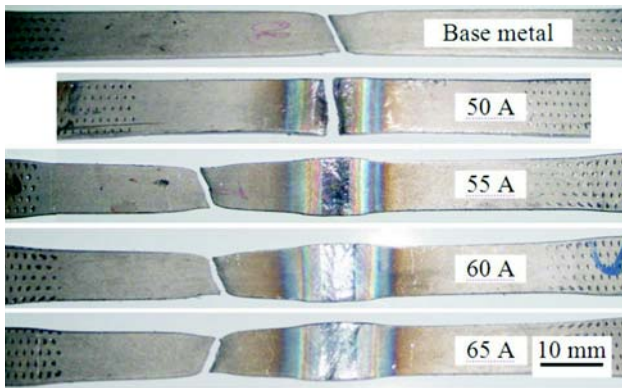

Fig. 5. Fracture photos of the specimens after tensile testing.

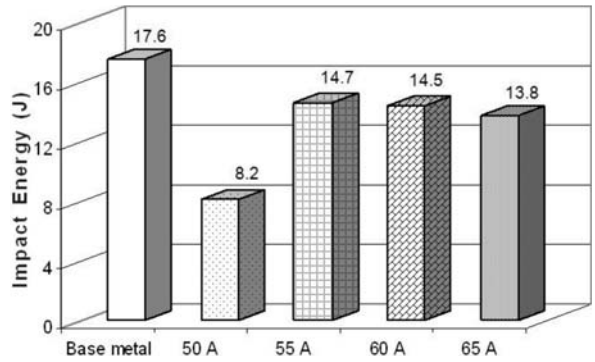

Fig. 6. Results of the Charpy impact test.

penetration was obtained for the specimens welded at 55, 60 and 65 A and therefore fractures took place in the base metal.

As the weld metal and base metal are essentially similar, they have the same modulus of elasticity and stretch uniformly as the load is applied in the elastic range. If the weld metal has higher yield stress, yield occurs first in the base metal at some point away from the weld, accompanied by necking. The true stress in this region increases more rapidly than the stress in the weld metal, since the necking is reducing the cross--section and fracture takes place in the base metal [26].

When the percent elongation values in Fig. 4 are compared, the highest elongation (65.2 %) is seen for the base metal and this is followed by the specimens welded at welding current of 55 (56.0 %), 60 (53.0 %) and 65 (50.8 %) A. Similar to the ultimate tensile strength values, the lowest percent elongation (16.4 %) value is seen for the specimen welded at 50 A welding current.

When a comparison is made between the ultimate tensile strength and elongation of the specimens (except from that welded at 50 A), considerable variation in the ultimate tensile strength values are not seen. However, the elongation decreases noticeably with increasing welding current. These decreases in the elongation can be attributed to increased hardness values with increasing welding current, Fig. 3.

Figure 5 indicates little deformation in the weld metal and HAZ while noticeable reductions are observed at the areas next to the weld metal and HAZ. It can be inferred that increasing welding current in the weld zone increased the heat input and this, in turn, enlarged the weld zone. It was noticed that enlarged weld zone reduced the elongation and at the same time caused it to take place in a narrow area.

3.4. Impact test

The results of the Charpy impact tests are illustrated in Fig. 6. It can be seen from Fig. 6 that the base metal has the highest absorbed impact energy than all the other welded specimens. The Charpy impact test results show that 8.2, 14.7, 14.5, and 13.8 J impact energies are required for the specimens welded at 50, 55, 60, and 65 A welding currents, respectively. When these results are examined, it is seen that very low impact fracture toughness was obtained for the specimen welded at 50 A welding current due to inadequate penetration. In addition, a decrease in the fracture toughness value with increasing welding current was observed. This decrease in the toughness can be explained by the impurity elements diffused into the weld metal. Barreda et al. [41] reported that titanium at temperatures above 350 ℃, and particularly in a molten state, was known to be very reactive towards most atmospheric gases such as oxygen, nitrogen, carbon, or hydrogen. These interstitial elements reduce ductility and toughness, while increasing strength and hardness.

3.5. Microstructure of welded joints

The images in Fig. 7 are optical micrographs of the (a) base metal, (b) base metal-heat affected zone and (c–f) fusion zones. Figure 7a shows the optical microscope image of the original CP-Ti. It is seen from this image that the microstructure consists of fine equiaxed α (alpha) grains. In the published literature [14, 41], microstructural characterisation of the joint showed the transition of microstructures from an equiaxed to an acicular microstructure. Titanium undergoes an allotropic phase transformation at 882 ℃ (alpha (HCP) $\rightleftharpoons$ beta (BCC)). During welding, the material in the fusion zone is heated to 882 ℃ or higher, resulting in transformation to β phase. As the weld cools through the β transus, the cooling rate from the β phase field has a controlling influence on the resulting microstructure in a CP-Ti [19].

Figure 7b shows the microstructure of the HAZ and fusion zone. Different microstructures are seen for the HAZ and fusion zone. These differences in the micro-

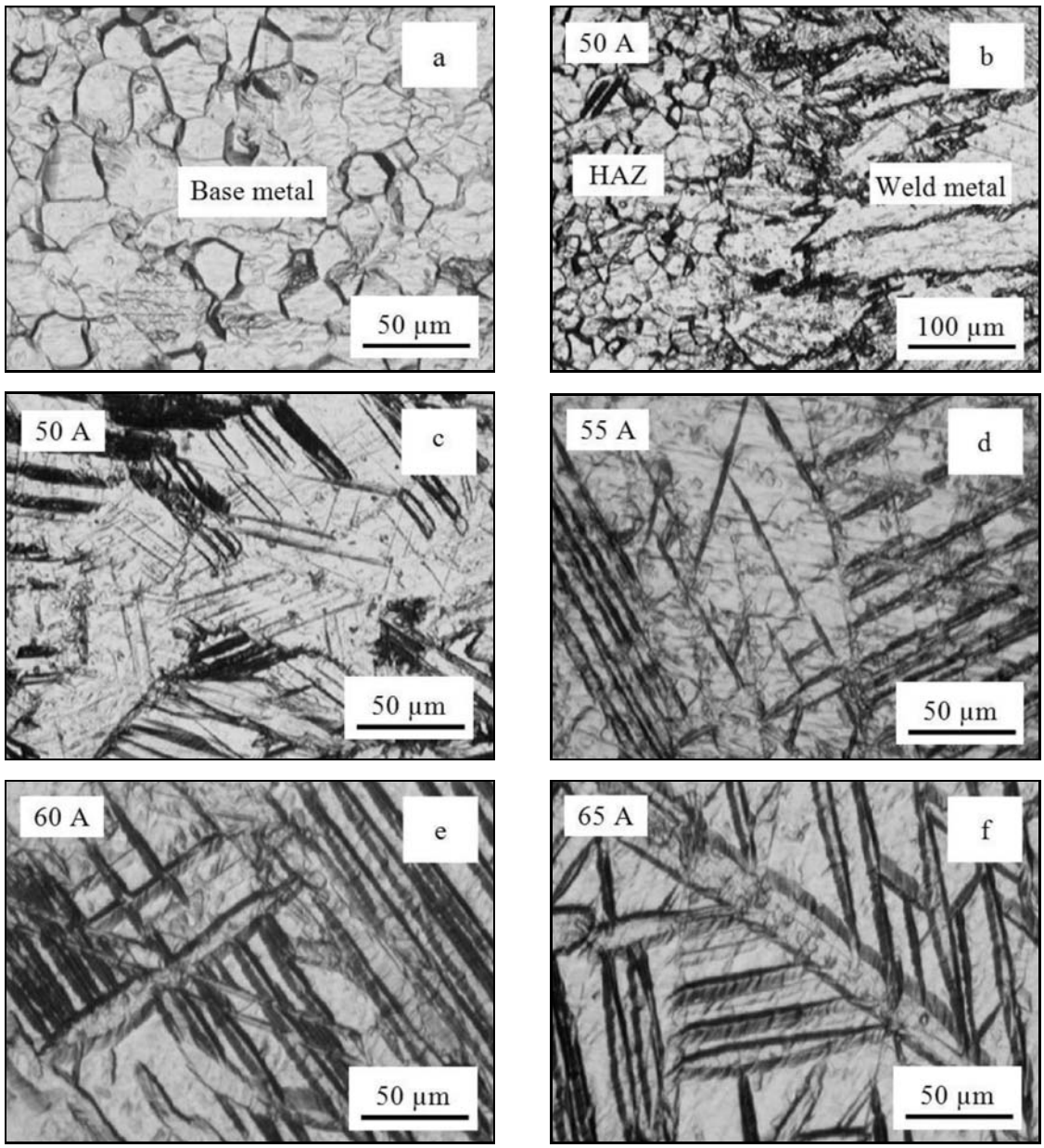

Fig. 7. Microstructures of (a) base metal, (b) base metal-heat affected zone and (c–f) weld metal.

structure can be attributed to different cooling rates [8]. The microstructure is the serrated alpha characterised by irregular grain size and jagged grain boundaries. The temperature of weld metal must be significantly higher than that of the HAZ during welding. Hence, the microstructure in the weld metal after air-cooling contained mainly acicular α and β with large prior β grain boundaries, as observed in Fig. 7b. It is now clear that the two zones in the welded joint have markedly different microstructures due to the temperature variations during welding and cooling processes [20]. Unfortunately, welding of titanium and its alloy leads to grain coarsening at the fusion zone and heat affected zone. Weld fusion zones typically exhibit coarse columnar grains because of the prevailing thermal conditions during weld metal solidification [1, 21].

Figures 7c–f show the details of the weld metal microstructure depending on the welding current, dominated by acicular alpha, coarse serrated alpha and twins. In addition, our results show that the microstructures of all the welded joints are essentially similar. The appearance of the twins is the distinct microstructural feature in the weld metal. These twins with different size and random orientation are found in the weld metal, especially near the weld centreline [19].

4. Conclusions

i) Titanium plates were joined successfully by

plasma arc welding method at various welding currents without filler metal using a single pass metal. The welded joint strength was found to be at least as much as that of the base metal when suitable welding current was used.

ii) The hardness values of the weld metal and HAZ were marginally higher than that of the base metal. Increasing welding current increased the hardness of weld metal and HAZ.

iii) The highest impact strength was obtained for the specimen welded at 55 A welding current.

iv) Acicular alpha and twins with different sizes dominated all of the weld metal microstructures.

References

[1] KAHRAMAN, N.—GULENÇ, B.—FINDIK, F.: Int. J. Impact Eng., *34*, 2007, p. 1423. doi:10.1016/j.ijimpeng.2006.08.003

[2] HE, L. B.—LI, L. M.—HAO, H. W.—WU, M. S.—ZHOU, R. L.: Sci. Technol. Weld. Joining, *11*, 2006, p. 72. doi:10.1179/174329306X77083

[3] BABU, N. K.—RAMAN, S. G. S.: Sci. Technol. Weld. Joining, *11*, 2006, p. 442. doi:10.1179/174329306X120750

[4] SOUL, F. A.—ZHANG, Y. H.: Sci. Technol. Weld. Joining, *11*, 2006, p. 688. doi:10.1179/174329306X147715

[5] BALASUBRAMANIAN, M.—JAYABALAN, V.—BALASUBRAMANIAN, V.: J. Mater. Process. Tech., *196*, 2008, p. 222. doi:10.1016/j.jmatprotec.2007.05.039

[6] ZHANG, Y.—SATO, Y. S.—KOKAWA, H.—PARK, S. H. C.—HIRANO, S.: Mat. Sci. Eng. A, *488*, 2008, p. 25. doi:10.1016/j.msea.2007.10.062

[7] BALASUBRAMANIAN, V.—JAYABALAN, V.—BALASUBRAMANIAN, M.: Mater. Design, *29*, 2008, p. 1459. doi:10.1016/j.matdes.2007.07.007

[8] SARESH, N.—PILLAI, M. G.—MATHEW, J.: J. Mater. Process. Tech., *192*, 2007, p. 83. doi:10.1016/j.jmatprotec.2007.04.048

[9] KAHRAMAN, N.—GULENÇ, B.—FINDIK, F.: J. Mater. Process. Tech., *169*, 2005, p. 127.

[10] KAHRAMAN, N.—GULENÇ, B.: J. Mater. Sci. Technol., *21*, 2005, p. 743.

[11] BOYER, R.: Mat. Sci. Eng. A, *213*, 1996, p. 103. doi:10.1016/0921-5093(96)10233-1

[12] SHANJIN, L.—YANG, W.: Opt. Laser Eng., *44*, 2006, p. 1067. doi:10.1016/j.optlaseng.2005.09.003

[13] ATASOY, E.—KAHRAMAN, N.: Mater. Charact., *59*, 2008, p. 1481. doi:10.1016/j.matchar.2008.01.015

[14] KAHRAMAN, N.: Mater. Design, *28*, 2007, p. 420. doi:10.1016/j.matdes.2005.09.010

[15] APARICIO, C.—GIL, F. J.—FONSECA, C.—BARBOSA, M.—PLANELL, J. A.: Biomaterials, *24*, 2003, p. 263. doi:10.1016/S0142-9612(02)00314-9

[16] HUANG, H. H.: Biomaterials, *23*, 2002, p. 59. doi:10.1016/S0142-9612(01)00079-5

[17] LIU, J.—WATANABE, I.—YOSHIDA, K.—ATSUTA, M.: Dent. Mater., *18*, 2002, p. 143. doi:10.1016/S0109-5641(01)00033-1

[18] LEE, W. B.—LEE, C. Y.—CHANG, W. S.—YEON, Y. M.—JUNG, S. B.: Mater. Lett., *9*, 2005, p. 3315. doi:10.1016/j.matlet.2005.05.064

[19] LI, C.—MUNEHARUA, K.—TAKAO, S.—KOUJI, H.: Mater. Design, *30*, 2009, p. 109. doi:10.1016/j.matdes.2008.04.043

[20] ZHOU, W.—CHEW, K. G.: Mat. Sci. Eng. A, *347*, 2003, p. 180. doi:10.1016/S0921-5093(02)00596-8

[21] BALASUBRAMANIAN, M.—JAYABALAN, V.—BALASUBRAMANIAN, V.: Mater. Design, *29*, 2008, p. 1359.

[22] YUNLIAN, Q.—JU, D.—QUAN, H.—LIYING, Z.: Mat. Sci. Eng. A, *280*, 2000, p. 177. doi:10.1016/S0921-5093(99)00662-0

[23] ZHANG, J. X.—XUE, Y.—GONG, S. L.: Sci. Technol. Weld. Joining, *10*, 2005, p. 643. doi:10.1179/174329305X48374

[24] WANG, Y.—ZHAO, P.: Int. J. Pres. Ves. Pip., *78*, 2001, p. 43. doi:10.1016/S0308-0161(00)00085-5

[25] YIN, F.—HU, S.—YU, C.—LI, L.: Comp. Mater. Sci., *40*, 2007, p. 389. doi:10.1016/j.commatsci.2007.01.008

[26] GOURD, L. M.: Principles of Welding Technology. Third ed. London, British Library Cataloguing in Publication Data 1995.

[27] OTERO, U. E.—UTRILLA, M. V.—MUNEZ, C. J.: J. Mater. Process. Tech., *182*, 2007, p. 624.

[28] JEFFUS, L.—JOHNSON, H. V.: Welding Principles and Applications. 2nd ed. New York, Delmar Publishers Inc. 1988.

[29] HARIS, D. I.: Plasma Arc Welding. ASM Handbook, Welding, Brazing and Soldering. Vol. 6. Materials Park, ASM International 2000.

[30] KURT, B.—ORHAN, N.—SOMUNKIRAN, I.—KAYA, M.: Mater. Design, *30*, 2009, p. 661.

[31] ALTHOUSE, D. A.—TURNGUIST, C. H.—BOWDITCH, W. A.—BOWDITCH, K. E.: Modern Welding. Tinley Park, IL, The Goodheart-Willcox Company Inc. 1988.

[32] CORREA, E. O.—COSTA, S. C.—SANTOS, J. N.: J. Mater. Process. Tech., *198*, 2008, p. 323.

[33] WANG, Y.—CHEN, Q.: J. Mater. Process. Tech., *120*, 2002, p. 270.

[34] SACKS, R. J.: Essentials of Welding. Macmillan, California, Glencoe Publishing Company, Inc. 1984.

[35] JIANG, J.—ZHANG, Z.: J. Alloy Compd., *466*, 2008, p. 368. doi:10.1016/j.jallcom.2007.11.034

[36] WANG, H. X.—WEI, Y. H.—YANG, C. L.: Comp. Mater. Sci., *40*, 2007, p. 213.

[37] LEI, Y. C.—YUAN, W. J.—CHEN, X. Z.—ZHU, F.—CHENG, X. N. T.: Nonferr. Metal Soc., *17*, 2007, p. 313. doi:10.1016/S1003-6326(07)60091-0

[38] LANGFORD, G. J.: Welding J., *47*, 1968, p. 102.

[39] LANGFORD, G. J.: Welding J., *45*, 1966, p. 811.

[40] WOOLCOCK, A.—RUCK, R. J.: Metal Construct., *10*, 1978, p. 576.

[41] BARREDA, J. L.—SANTAMARIA, F.—AZPIROZ, X.—IRISARRI, A. M.—VARONA, J. M.: Vacuum, *62*, 2001, p. 143. doi:10.1016/S0042-207X(00)00454-1